J Solid State Electrochem (2013) 17:2001–2008
DOI 10.1007/s10008-013-2053-z

ORIGINAL PAPER

Structural and optical properties of tripod-like ZnO thin film and its application in dye-sensitized solar cell

Lal Bahadur · Suman Kushwaha

Received: 6 September 2012 / Revised: 23 February 2013 / Accepted: 25 February 2013 / Published online: 14 March 2013

Abstract In this work, we have synthesized Zinc oxide (ZnO) tripods and used its thin film as photoanode in dye-sensitized solar cells. SEM micrographs of the as-prepared sample of ZnO confirmed tripod-like morphology consisting of three cylindrical arms with well-defined ends, joined at a common core. The prepared sample of ZnO tripods was further characterized by EDX, XRD, UV-VIS, and FTIR. The dye N719-sensitized solar cell fabricated with photoanode of ZnO prepared in this work provided the open-circuit photo voltage (V_{oc})=0.558 V, short-circuit photocurrent (J_{sc})=6.368 mA cm^{-2}, fill factor (FF)=0.50, and total conversion efficiency (η)=0.88 % under full light illumination (intensity 200 mW cm^{-2}). When cell was illuminated by visible light (150 mW/cm^2), V_{oc}=0.546 V, J_{sc}=4.437 mA/cm^2, FF=0.54, and η=0.88 % were obtained.

Keywords DSSC · ZnO tripods · Thin film · SEM

Introduction

Zinc oxide (ZnO) is distinguished for its multiple properties like semiconducting, piezoelectric or pyroelectric properties, wear resistance, microwave absorption, etc. With hexagonal wurtzite structure, ZnO has a wideband gap (E_g=3.3 eV) and higher exciton binding energy ex E_b= 60 meV at room temperature compared to other wideband emission materials [1, 2] such as ZnSe (E_g=2.7 eV, ex E_b= 20 meV) and GaN (E_g=3.4 eV, ex E_b=21 meV). ZnO have been extensively studied because of its potential applications in various fields such as gas sensor, solar cells, photodetectors, light emitting diodes [3-9], and laser systems, etc. An important advantage of ZnO over TiO_2 is that it can be synthesized by applying a wide range of synthesis techniques [10-13] to obtain a great variety of different morphologies and nanostructures. Various chemical and physical methods have been applied for creating ZnO nanostructures. For instance, high temperature vapor–liquid–solid growth with the use of catalysts, pulsed laser deposition, electrochemical deposition in porous membranes, metal vapor transport using Zn sources, physical vapor transport using ZnO and graphite powders, chemical vapor deposition using zinc acetylacetonate hydrate, thermal oxidation of ZnS, metalorganic chemical vapor deposition, aqueous chemical growth, and sol-gel have been reported among other techniques [14-24]. During the past few years, attention has been focused on one-dimensional (1D) nanostructure materials, such as nanowires and nanorods, due to their fundamental importance and wide range of potential applications in nano devices [25, 26]. Various methods have been developed for the preparation of 1D nanostructure in order to obtain nanowires or nanorods of the desired materials [27-32].

The 1D ZnO nanostructures are of interest for their applications in dye-sensitized solar cells (DSSCs) [33] and also because they exhibit significantly improved electron transport compared to that in porous films. One-dimensional ZnO nanostructures were prepared by several groups, some of which are discussed here. Yan et al. synthesized ZnO tetrapods using a chemical vapor transport and condensation system in which Zn powder was used as Zn source [34]. Liu et al. prepared ZnO tetrapods, nanotetraspikes, and nanowires using aqueous solution of KOH and Zn foil [35]. Zhong et al. prepared ZnO tetrapods in a horizontal tube furnace by evaporating Zinc at 950 °C in the flow of humid argon gas [36]. Chen et al. [37] prepared tetrapods of ZnO by annealing Zn foil at higher temperature. Unlike these

L. Bahadur (✉) · S. Kushwaha
Department of Chemistry, Faculty of Science,
Banaras Hindu University, Varanasi 221005, India
e-mail: lbahadur@bhu.ac.in

methods, in the present work, one-dimensional ZnO with tripod-like morphology has been synthesized in a horizontal tube furnace by heating dried zinc oxide paste at 550 °C in the stream of hydrogen gas. From these ZnO tripods, thin films have been prepared and used as photoanode in DSSCs.

It is pertinent to elaborate a little further why we chose to synthesize tripods instead of tetrapods or other branched structures. Our attempt was to synthesize one-dimensional ZnO nanostructures which could significantly reduce the numerous electron-hopping interjunction existing in the porous films consisting of spherical grain type nanoparticles. Tripods are likely to meet this requirement because their branches equip them with the ability to form mechanically robust network films for easy transport of injected electrons from the excited dye molecules to the substrate (fluorine-doped tin oxide (FTO)) through this network. However, thin film consisting of tripods would have smaller surface area as compared to that of a film composed of spherical grain type particles. Thin films composed of tetrapods or other branched structures, though, may still be better for the electron transport but the effective surface area is likely to reduce further which may have adverse effect on dye loading on the surface of the film. Hence, tripod structure is a good compromise to have a network for easy electron transport without reducing the surface area to a greater extent.

Experimental

Materials

All the chemicals, ZnO (99.9 %), sodium hydroxide, lithium hydroxide, 1-butanol, and LiI were purchased from Sigma-Aldrich and have been used without further purification. N719 dye and 60 μm thick heat shrinkable sealing sheet (SX 1170-60) were purchased from Solaronix. Molecular iodine (I_2) was purchased from BDH Chemicals Pvt. Ltd, India. FTO-coated glass substrates (thickness=2.2 mm and surface resistance 15 Ω/□) obtained from Pilkington, USA, were used for making ZnO thin films.

Preparation of tripod-like ZnO powder and its thin film

The experimental setup used for the preparation of ZnO tripods is shown schematically in Fig. 1a. The expected process of evolution of ZnO tripods from ZnO microspheres are shown in Fig. 1b [38-40]. In a typical synthesis process, 0.5 g of high purity ZnO was pretreated with 0.12 g NaOH and 0.25 g LiOH H_2O and thoroughly mixed. The mixture was then placed in the central region of the digitally controlled horizontal tube furnace. Hydrogen carrier gas was then introduced into the tube at a continuous but slow flow rate while the temperature of the furnace was maintained at 550 °C for 3.5 h. To obtain an accurate estimation of the growth temperature, the temperature gradient of the tube furnace was calibrated using inbuilt thermocouple. The reaction of ZnO with alkali results in $[Zn(OH)_4]^{2-}$ ion which changes first to $Zn(OH)_2$ and on subsequent heating process, $Zn(OH)_2$ is converted into ZnO clusters. At a high temperature of 550 °C, nucleation centers are formed on ZnO surface. With increasing heating time (3.5 h), the structure of ZnO crystals gradually transforms into its thermodynamically preferred configuration, which could be pod like.

For preparing thin films of ZnO tripods, 0.3 g of ZnO tripods sample was first mixed in 8 mL of 1-butanol to form a sufficiently viscous paste. The paste prepared with other proportions of ZnO and 1-butanol or with the use of other solvents like methanol, ethanol, and surfactant triton-X did not give satisfactory result (adherent and uniform films). The doctor's blade technique was employed to spread the paste onto a conductive glass substrate. Prior to deposition,

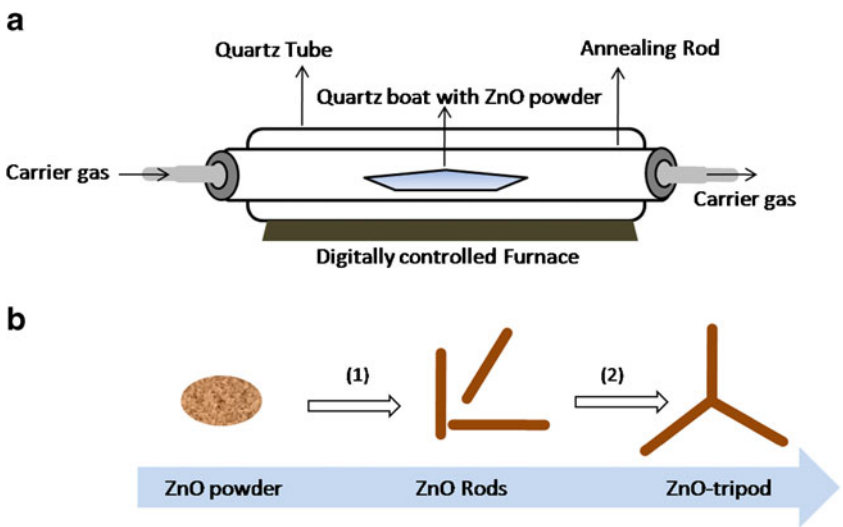

Fig. 1 (**a**) Schematic diagram of the experimental setup used for synthesizing ZnO tripods using H_2 as carrier gas and (**b**) schematic presentation of two-step process expected to be involved in the growth of ZnO tripod

Scheme 1 Schematic diagram of sandwich-type dye-sensitized solar cell

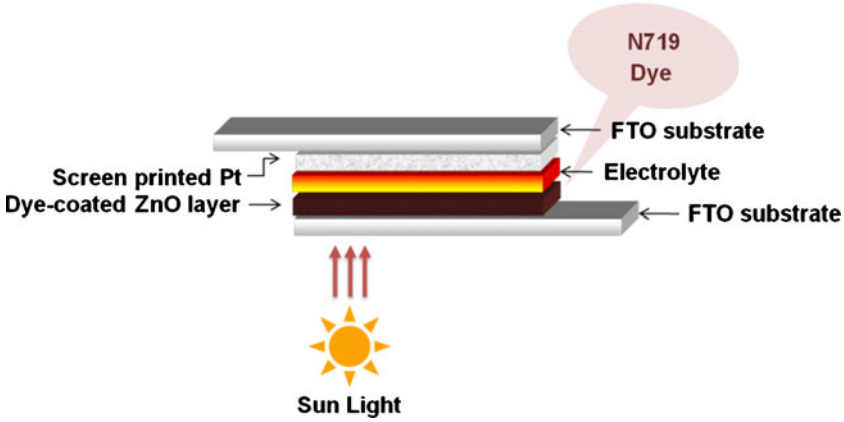

substrate was ultrasonically cleaned and kept in an oven at 80 °C for 30 min. Substrates were covered on all edges with adhesive tape to control the thickness of the ZnO film and to provide noncoated areas for electrical contact. After drying them in vacuum oven at room temperature, the films (~6 μm thickness) were immersed overnight in 0.1 mM ethanol solution of N719 dye for its adsorption onto surface of ZnO thin film. Platinum counter electrode was prepared by deposition of Pt catalyst T/SP paste (purchased from Solaronix SA) on another conductive glass by screen printing method and annealed at 400 °C for half an hour in air.

To assemble the cell, a U-shaped frame of hot-melt sheet (SX1170-60, 50 μm thick, Solaronix) was put over the photoelectrode for keeping the space between the electrodes for cell electrolyte and also for sealing the cell assembly (schematically shown in Scheme 1). The counter electrode was then placed over and sealed with the photoanode by heating the assembly at ~80 °C. The electrolyte solution composed of LiI (0.5 M), I_2 (0.05 M) in propylene carbonate was introduced into the cell by capillary action and then sealed properly. Propylene carbonate is frequently used in many electrochemical investigations because of its wide potential window. Furthermore, its donor number, dielectric constant, and boiling point are higher than acetonitrile which are likely to improve the cell outputs (particularly V_{oc} due to higher donor number) and there would be lesser chance of evaporation of the solvent (due to high boiling point). In addition to this, it was already reported in our earlier publication [40] that cell performance was better with the use of propylene carbonate than acetonitrile. Because of these reasons, propylene carbonate was used as the medium of cell electrolyte.

Characterization equipments

The scanning electron microscopy (SEM) images of ZnO sample were recorded soon after its preparation using a field emission scanning electron microscopy (quanta200 FEG) and analysis of elemental composition was done by Energy Dispersive x-ray analysis (EDX). The crystallinity of tripod-shaped ZnO was determined using X-ray diffraction measurement (XRD, Model 3000, Seifert, Germany). The absorption studies of the samples were carried out by Shimadzu UV-1700 spectrophotometer. Photocurrent potential measurements were made using a bipotentiostat (model no. AFRDE4E, Pine Instrument Company, USA) and a

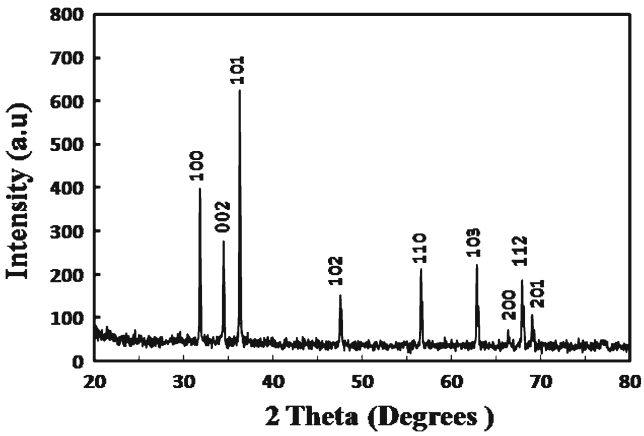

Fig. 2 XRD pattern of the ZnO tripod-like nanostructure

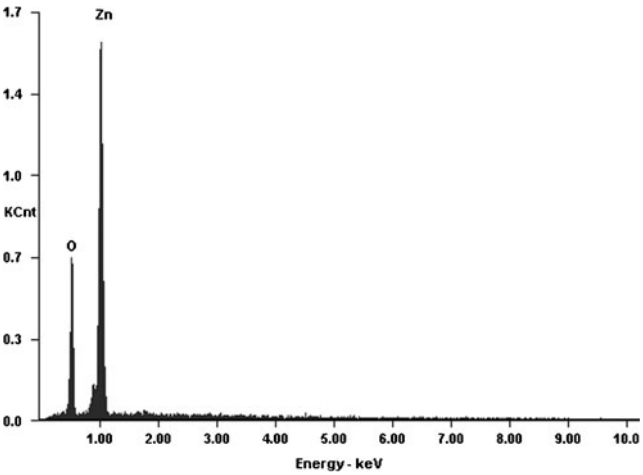

Fig. 3 EDX spectrum of the nanorod showing its constituents

computer controlled e-corder (model no. 201, eDAQ, Australia). A 150 W xenon arc lamp (lamp housing model no. 66057 and power supply model no. 68752, Oriel Corporation, USA) equipped with an infrared (IR) filter (water filter) was used as a light source for the illumination of photoelectrodes during photoelectrochemical measurements.

The semiconductor electrode was illuminated after passing the collimated light beam through a 6 in-long water column (to filter IR part of light) and condensing it with the help of fused silica lenses (Oriel Corporation, USA). This IR-filtered light is referred to as "white light" in the text. Whenever required, the UV part of the white light was cut off by using a long-pass filter (model no. 51280, Oriel Corporation, USA) and the resultant light obtained in this way is referred to as "visible light." The monochromatic light was obtained with the use of a monochromator (Oriel model no. 77250 equipped with model no. 7798 grating) and short-circuit photocurrent obtained under monochromatic light illumination was measured with the help of a digital multimeter (Philips model no. 2525).

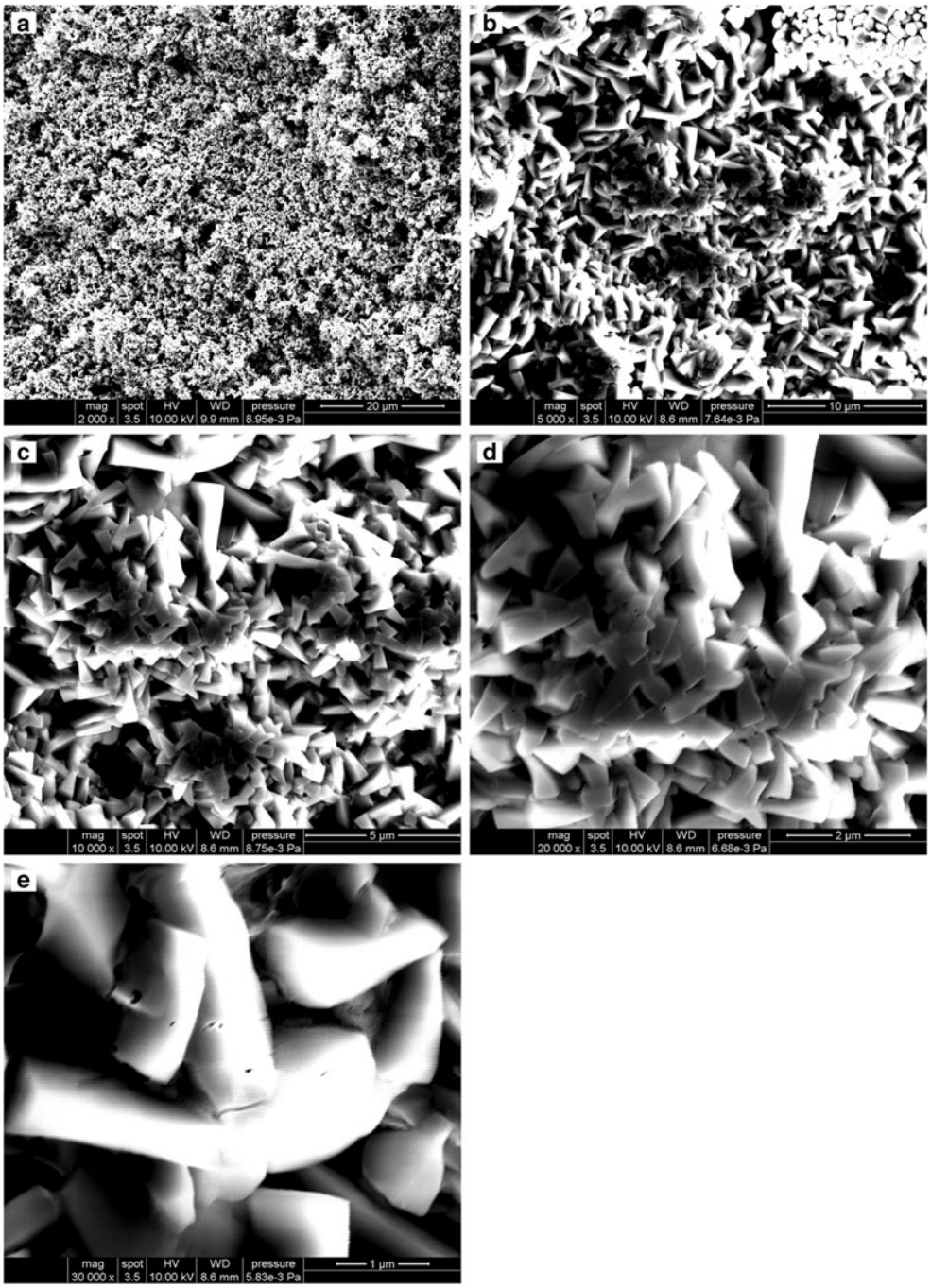

Fig. 4 SEM images of as-prepared ZnO sample taken at different magnifications:[**a**] ×2,000; [**b**] ×5,000; [**c**] ×10,000; [**d**] ×20,000; and [**e**] ×30,000

Methodology

The cell output parameters, namely, total conversion efficiency (η) and fill factor (FF) of the cell, were determined by using current–potential curve (J-V) obtained under illumination with white light (200 mW/cm^2) and visible light (150 mW/cm^2). The maximum power P_{max} was determined from current–potential curve by choosing a point on the curve corresponding to which the product of the current (J_{max}) and potential gives the maximum value (V_{max}). The fill factor and overall η were then calculated from the following equations:

$$\eta(\%) = \frac{J_{max}\ (A\ cm^{-2}) \times V_{max}(V)}{I_{inc}\ (W\ cm^{-2})} \times 100 \quad (1)$$

$$FF = \frac{J_{max} \times V_{max}}{J_{sc} \times V_{oc}} \quad (2)$$

where I_{inc} is the power of incident light.

The short-circuit photocurrent (J_{photo}) of the dye-sensitized cell was measured as a function of the wavelength of monochromatic light (λ) used for the illumination of the DSSC. From these values of J_{photo} (A/cm^2) and the intensity of the corresponding monochromatic light, I_{mono} (W/cm^2), the incident photon to current conversion efficiency (IPCE) was calculated at each excitation wavelength (λ, expressed in nm) using the following equation:

$$IPCE\ (\%) = \frac{1,240\ J_{photo}}{\lambda \times I_{mono}} \times 100 \quad (3)$$

Results and discussion

XRD and EDX analysis

Figure 2 shows the x-ray diffraction (XRD) pattern of tripod-like ZnO confirming the hexagonal crystal structure of ZnO. It exhibits diffraction peaks at (100), (002), (101), (102), (110), (103), (200), (112), and (201) with the peak (101) having the highest intensity. All these diffraction peaks are in agreement with the reported data in JCPDS card no. 36-1451 for hexagonal wurtzite phase of zinc oxide [35]. EDX measurement was made on an individual nano-rod arm of ZnO tripod and the result is shown in Fig. 3 wherein the peaks of Zn and O indicate that the nanostructure is without any impurity.

Surface morphology

The SEM images of as-prepared ZnO sample taken at different magnifications are shown in Fig. 4. It reveals that phase transition from ZnO grain particles to tripod-like ZnO nanostructures takes place during annealing. Highly magnified

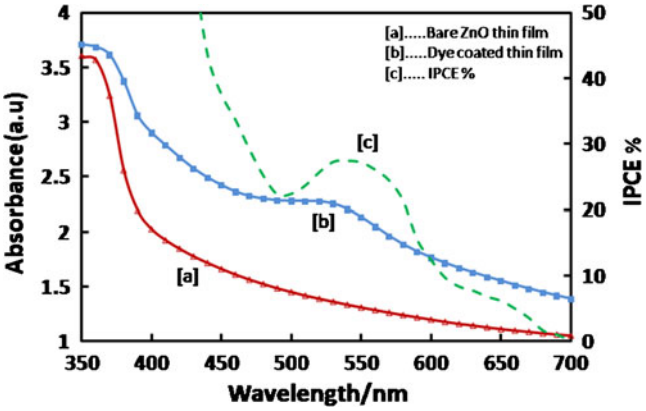

Fig. 5 UV-Vis absorption spectra of bare thin film of ZnO tripods [**a**] and dye N719-coated ZnO thin film [**b**]. The curve [**c**] shows the IPCE as a function of the wavelength of incident monochromatic light

SEM image shown in Fig. 4d (×20,000) exhibits mostly tripod-like structure. From Fig. 4e (×30,000), rough measurement of the size of the tripod-like nanostructures can be made. It is observed that it has thin arms less than a micron in length where as the diameter of each rod is about~500 nm. Hence, from SEM micrographs, it can be concluded that synthesized ZnO particles have tripod-like structure with uniform arm length and diameter which suggests that each arm grows preferentially along the crystal c-axis as suggested by Liu et al. [39].

Optical properties

Figure 5 (curve a) shows the absorption spectrum of the thin film of ZnO tripods. The absorption peak of ZnO tripods is around λ=373 nm (~3.33 eV), which is ascribed to the ground excitonic state. The observed ground state exciton energy (3.33 eV) is slightly red shifted compared to the free exciton energy in the bulk (3.37 eV). In comparison to that of bare thin film of ZnO tripods (curve a in Fig. 5), the spectral response of dye N719-coated ZnO film was greatly enhanced in the visible region (curve b in Fig. 5).

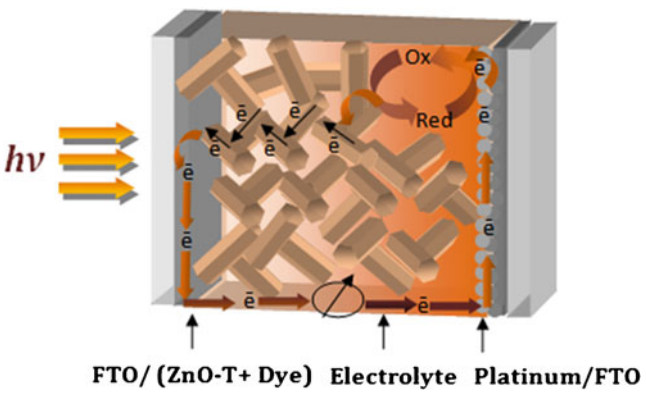

Fig. 6 Schematically showing the possible electron transport pathways across the dye-sensitized solar cell

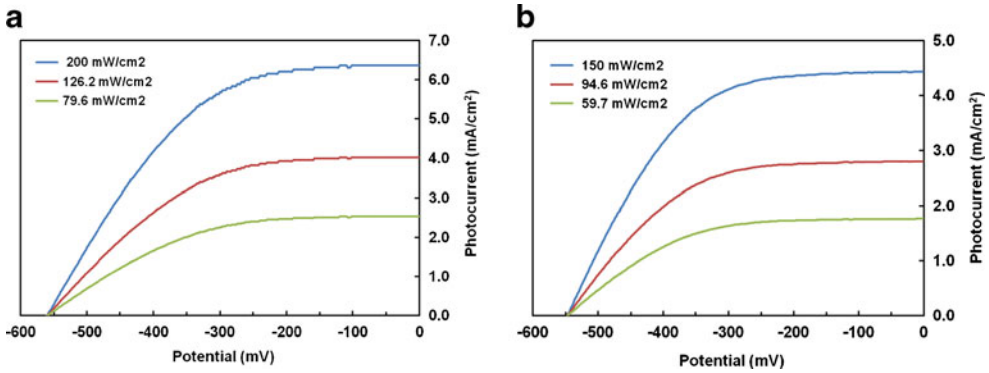

Fig. 7 Current–potential (*J-V*) curves for dye-sensitized solar cell illuminated by (**a**) white light and (**b**) visible light of different intensities

The short-circuit photocurrent (J_{photo}) of the dye-sensitized cell was measured as a function of the wavelength of monochromatic light (λ) used for the illumination of the semiconductor electrode. The IPCE spectrum (action spectra) thus obtained is shown as curve c in Fig. 5. The IPCE value for the present system was found to be 30 % at the characteristic wavelength of the dye (λ_{max}=535 nm).

Photovoltaic characteristics

Relative to thin film prepared from colloidal ZnO obtained from sol-gel method, electron transport is expected to be much easier in thin films composed of arrays of nanorod because latter case electrons can easily move from one arm to another arm of the tripod array (Fig. 6). The tripod-like structured thin film should exhibit better charge transport than nanoparticle films for the reason that the characteristic symmetrically branched structure of the nanotripods ensures that at least one of its three arms roughly points to the direction perpendicular to the conductive glass substrate. Therefore, the average number of inter junctions across which photo-injected electrons in the tripod-like film need to pass along the perpendicular direction in order to be collected at the anode has more chances [37].

Current–potential characteristics

The *J-V* of N719-sensitized ZnO-based DSSC was recorded under illumination with white light and visible light of different intensities and the results are shown in Fig. 7. Under illumination with white light of 200 mW/cm^2 intensity [Fig. 7a], the open-circuit cell voltage (V_{oc})=558 mV, short-circuit current J_{sc}=6.368 mA/cm^2, *FF*=0.50, and η=0.88 % were observed. When cell was illuminated with visible light (150 mW/cm^2) [Fig. 7b], the V_{oc}= 546 mV, J_{sc}=4.437 mA/cm^2, *FF*=0.54, and η=0.88 % were observed. Actual illuminated area of the working electrode was 0.19 cm^2. Since white light consists of UV part also (in addition to visible light), with the use of such light, both ZnO and dye would be excited and contribute to photocurrent. To obtain the photocurrent solely due to sensitizing dye, experiments were conducted under visible light illumination. So, the photocurrent shown in Fig. 7b can exclusively be ascribed to sensitization by dye. With the variation in intensity of light (white or visible), the J_{sc} was found to vary almost proportionally while V_{oc}, *FF*, and η remained almost unchanged (Table 1).

The overall performance of the DSSC fabricated with photoanode of ZnO synthesized during present work was satisfactory in terms of V_{oc}, J_{sc}, and *FF*, though conversion efficiency was low. This may be due to poor adherence of thin film on FTO-coated glass substrate (since film was not annealed) and small active surface area of the film (due to bigger particle size of the tripods) leading to poor adsorption of dye on ZnO surface structure.

Table 1 Cell output parameters derived from *J-V* curves (Fig. 8a and b)

Type of light	Intensity (mW/cm^2)	J_{sc} (mA/cm^2)	V_{oc} (mV)	*FF*	η (%)
White light	200.0	6.368	558	0.50	0.88
	126.2	4.018	558	0.50	0.88
	79.6	2.535	558	0.50	0.88
Visible light	150.0	4.437	546	0.54	0.88
	94.6	2.800	546	0.54	0.88
	59.7	1.766	546	0.54	0.88

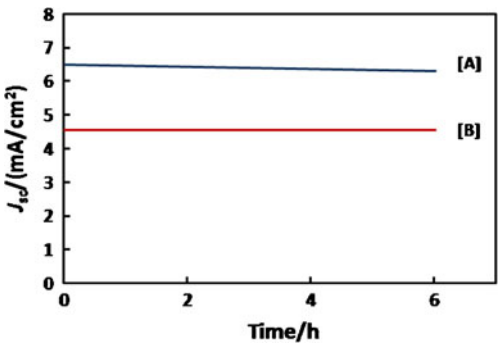

Fig. 8 The stability of photocurrent on prolong operation of the cell under illumination by [**A**] white light (200 mW/cm^2 and [**B**] visible light (150 mW/cm^2)

Stability of the photocurrent on prolong operation of the cell

The stability of the photocurrent on prolong operation (for a few hours) of the DSSC was studied and result is shown in Fig. 8. The dye-sensitized solar cell was illuminated with desired light and the short-circuit photocurrent was monitored for 6 h of continuous operation of the cell and the results are shown in Fig. 8. After 6 h of continuous illumination of the cell, not much reduction in photocurrent was observed particularly under visible light illumination.

Conclusion

In this work, ZnO with tripod-like nanostructures was prepared by employing a novel method and the same was used to make thin-film photoanodes. This electrode, sensitized with N719 dye, was in turn used in DSSC configuration to assess the quality of the tripod-like ZnO prepared during this work. With such cell under illumination with white light (200 mW/cm^2), J_{sc}=6.368 mA/cm^2, V_{oc}=558 mV, FF= 0.50, and η=0.88 % were obtained. Under visible light illumination (150 mW/cm^2), J_{sc}=4.437 mA/cm^2, V_{oc}= 546 mV, FF=0.54, and η=0.88 % were achieved. The J_{sc} and total conversion efficiency obtained in present investigation are not very encouraging in comparison to those reported by others [38]. This might be due to poor adherence of the ZnO film and large size of ZnO tripods synthesized. To increase the adherence of the film on the substrate, annealing at higher temperatures and the use of some binders can be tried but care needs to taken to keep the tripod structure intact. Furthermore, the particle size can possibly be reduced by hastening the reaction (allowing lesser time to grow the tripods) using some catalyst. These possibilities are being explored.

Acknowledgments Financial support from the Ministry of New and Renewable Energy (MNRE, New Delhi, India) and Council of Scientific and Industrial Research (CSIR, New Delhi) is gratefully acknowledged. Thanks are also due to Indian Institute of Technology, Banaras Hindu University, Varanasi, India for providing their facilities (XRD and SEM) during this work.

References

1. Tang ZK, Wong GKL, Yu P, Kawasaki M, Ohtomo A, Koinuma H, Segawa Y (1998) Room-temperature ultraviolet laser emission from self-assembled ZnO microcrystallite thin films. Appl Phys Lett 72:3270–3272
2. Ryu MK, Lee SH, Jang MS, Panin GN, Kang TN (2002) Post-growth annealing effect on structural and optical properties of ZnO films grown on GaAs substrates by the radio frequency magnetron sputtering technique. J Appl Phys 92:154–159
3. Bahadur L, Srivastava P (2003) Efficient photon-to-electron conversion with rhodamine 6 G-sensitized nanocrystalline n-ZnO thin film electrodes in acetonitrile solution. Sol Energy Mater Sol Cell 79:235–248
4. Kushwaha S, Bahadur L (2011) Characterization of some metal-free organic dyes as photosensitizer for nanocrystalline ZnO-based dye sensitized solar cells. Int J Hydrogen Energy 36:1162–1167
5. Kushwaha S, Bahadur L (2011) Characterization of synthetic Ni(II)—xylenol complex as a photosensitizer for wide-band gap ZnO semiconductor electrodes. Int J Photoenergy. doi:10.1155/2011/980560
6. Bahadur L, Kushwaha S (2012) Highly efficient nanocrystalline ZnO thin films prepared by a novel method and their application in dye-sensitized solar cells. Appl Phys A: Mater Sci Process 109:655–663
7. Kushwaha S, Bahadur L (2012) Natural alkannin and anthocyanin as photosensitizers for dye-sensitized solar cells. Proc SCES (2012) Student conf, held at Allahabad, Uttar Pradesh, doi:10.1109/SCES.2012.6199084
8. Liu Y, Gorla CR, Liang S, Emanetoglu N, Lu Y, Shen H, Wraback M (2000) Ultraviolet detectors based on epitaxial ZnO films grown by MOCVD. J Electron Mater 29:69–74
9. Naseri N, Yousefi M, Moshfegh AZ (2011) A comparative study on photoelectrochemical activity of ZnO/TiO_2 and TiO_2/ZnO nano-layer systems under visible irradiation. Sol Energy 85:1972–1978
10. Lu L, Li R, Fan K, Peng T (2010) Effects of annealing conditions on the photoelectrochemical properties of dye-sensitized solar cells made with ZnO nanoparticles. Sol Energy 84:844–853
11. Chen H, Li W, Liu H, Zhu L (2010) A suitable deposition method of CdS for high performance CdS-sensitized ZnO electrodes: sequential chemical bath deposition. Sol Energy 84:1201–1207
12. Pawar RC, Shaikh JS, Babar AA, Dhere PM, Patil PS (2011) Aqueous chemical growth of ZnO disks, rods, spindles, and flowers: pH dependency and photoelectrochemical properties. Sol Energy 85:1119–1127
13. Hames Y, Alpaslan Z, Kösemen A, San SE, Yerli Y (2010) Electrochemically grown ZnO nanorods for hybrid solar cell applications. Sol Energy 84:426–431
14. Huang HM, Wu Y, Feick H, Tran N, Weber E, Yang P (2001) Catalytic growth of zinc oxide nanowires by vapor transport. Adv Mater 13:113–146
15. Choi JH, Tabata H, Kawai T (2001) Fabrication and optoelectronic properties of a transparent ZnO homostructural light-emitting diode. J Cryst Growth 226:493–500
16. Liu CH, Zapien JA, Yao Y, Meng XM, Lee CS, Lee FSS (2003) High-density, ordered ultraviolet light-emitting ZnO nanowire arrays. Adv Mater 15:838–841
17. Lyu SC, Zhang Y, Ruh H, Lee HJ, Shim HW, Suh EK, Lee CJ (2002) Low temperature growth and photoluminescence of well-aligned zinc oxide nanowires. Chem Phys Lett 363:134–138
18. Yao BD, Chen YF, Wang N (2002) Formation of ZnO nanostructures by a simple way of thermal evaporation. Appl Phys Lett 81:757–759
19. Wu JJ, Liu SC (2002) Catalyst-free growth and characterization of ZnO nanorods. J Phys Chem B 106:9546–9551
20. Zhang XT, Liu YC, Zhang LG, Zhang JY, Lu YM, Shen DZ, Xu W, Zhong GZ, Fan XW, Kong XG (2002) Structure and optically pumped lasing from nanocrystalline ZnO thin films prepared by thermal oxidation of ZnS thin films. J Appl Phys 92:3293–3298
21. Kim SW, Fujita S, Fujita S (2002) Self-organized ZnO quantum dots on SiO_2/Si substrates by metalorganic chemical vapor deposition. Appl Phys Lett 81:5036–5065
22. Vayssieres L (2003) Growth of arrayed nanorods and nanowires of ZnO from aqueous solutions. Adv Mater 15:464–466
23. Hirano S, Kato K (1988) Formation of $LiNbO_3$ films by hydrolysis of metal alkoxides. J Non-Cryst Solids 10:538–541

24. Arfsten NJ (1984) Sol-gel derived transparent IR-reflecting ITO semiconductor coatings and future applications. J Non-Cryst Solids 63:243–249
25. Hu JT, Odom TW, Lieber CM (1999) Chemistry and physics in one dimension: synthesis and properties of nanowires and nanotubes. Acc Chem Res 32:435–439
26. Xia Y, Yang P, Sun Y, Wu Y, Mayers B, Gates B, Yin Y, Kim F, Yan H (2003) One-dimensional nanostructures: synthesis, characterization, and applications. Adv Mater 15:353–389
27. Wu Y, Yang P (2000) Germanium nanowire growth via simple vapor transport. Chem Mater 12:605–607
28. Chen CC, Yeh CC (2000) Large-scale catalytic synthesis of crystalline gallium nitride nanowires. Adv Mater 12:738–741
29. Bai ZB, Yu DP, Zhang HZ, Ding Y, Gai XZ, Hang QL, Xiong GC, Feng SQ (1999) Nano-scale GeO_2 wires synthesized by physical evaporation. Chem Phys Lett 303:311–314
30. Yazawa M, Koguchi M, Muto A, Ozawa M, Hiruma K (1992) Effect of one monolayer of surface gold atoms on the epitaxial growth of In as nanowhiskers. Appl Phys Lett 61:2051–2053
31. Choi YC, Kim WS, Park YS, Lee SM, Bae DJ, Lee YH, Park G-S, Choi WB, Lee NS, Kim JM (2000) Catalytic growth of β-Ga2O3 nanowires by arc discharge. Adv Mater 12:746–749
32. Duan XF, Leiber CM (2000) General synthesis of compound semiconductor nanowires. Adv Mater 12:298–302
33. Chen Z, Shan Z, Cao M, Lun L, Mao S (2004) ZnO nanotetrapods. Nanotechnology 15:365–367
34. Yan H, He R, Pham J, Yang P (2003) Morphogenesis of one-dimensional ZnO nano- and microcrystals. Adv Mater 15:402–405
35. Liu F, Cao PJ, Zhang HR, Li JQ, Gao HJ (2004) Controlled self-assembled nanoaeroplanes, nanocombs, and tetrapod-like networks of zinc oxide. Nanotechnology 15:949–952
36. Zhong Y, Djurisic AB, Hsu YF, Wong KS, Brauer G, Ling CC, Chan WK (2008) Exceptionally long exciton photoluminescence lifetime in ZnO tetrapods. J Phys Chem C 112:16286–16295
37. Chen W, Zhang H, Hsing IM, Yang S (2009) A new photoanode architecture of dye sensitized solar cell based on ZnO nanotetrapods with no need for calcinations. Electrochem Commun 11:1057–1060
38. Chen W, Yang S (2011) Dye-sensitized solar cells based on ZnO nanotetrapods. Front Optoelectron China 1:24–44
39. Liu Y, Chen Z, Kang Z, Bello I, Fan X, Shafiq I, Zhang W, Lee ST (2008) Self-catalytic synthesis of ZnO tetrapods, nanotetraspikes, and nanowires in air at atmospheric pressure. J Phys Chem C 112:9214–9218
40. Bahadur L, Rao TN (1995) Photoelectrochemical investigations on particulate ZnO thin film electrodes in non-aqueous solvents. J Photochem Photobiol A Chem 3:233–240